memo

Washington Department of Fish and Wildlife

To: Erik Lesko and Chris Karchesky, PacifiCorp
From: Kale Bentley, WDFW
CC: Lewis ATS
Date: April 19, 2024
Subject: Estimates of abundance for adult Chinook downstream of Merwin Dam, 2023

Executive Summary
In 2023, the Washington Department of Fish and Wildlife (WDFW) conducted weekly mark-recapture surveys from September 5th through December 26th, 2023. Across all surveys, 6,262 unique Chinook carcasses were recovered of which 2,047 were tagged and 780 were recaptured. Flows and visibility were generally favorable from September through November and PacifiCorp provided four of the five requested drawdowns during November. However, heavy rain and subsequent dam operations resulted in sustained lower river flows greater than 10,000 CFS for approximately 2 ½ weeks, which resulted in surveys being canceled the first week of December and a low number of carcasses recoveries the second week of December. An additional drawdown during the third week of December dramatically improved survey conditions resulting in hundreds of recoveries, including dozens of recaptures that were originally tagged in November, which helped provide a robust data set that encompassed the entire run. Using a Jolly-Seber (JS) open population model, the total estimates of abundance (mean; %CV) for spring-, fall- (tule), and late fall-run (bright) Chinook salmon were 109 (77%), 3,044 (13%), and 8,368 (6%), respectively. The proportion of estimated abundance that were hatchery-origin spawners (pHOS) for the three run-types was estimated to be 0.74, 0.58, and 0.02, respectively.

Project Overview
WDFW has been conducting spawning ground surveys for adult Chinook salmon in the mainstem North Fork (NF) Lewis River downstream of Merwin Dam for over five decades. Over this time, the methods used to assess the status of NF Lewis Chinook have varied. Since 2013, WDFW has been implementing weekly mark-recapture surveys using carcasses recovered from the river and adjacent streambanks to estimate the abundance and composition of Chinook salmon spawners throughout their entire spatial and temporal extent each year. The estimates of abundance and composition are used by WDFW, NOAA, and other entities to assess the status and trend of NF Lewis populations of Chinook, which represent three of the 32 historical independent populations with the Lower Columbia River (LCR) Chinook salmon Evolutionarily Significant Unit (ESU). The monitoring of wild fall Chinook spawner populations in the NF Lewis River is also a requirement of the Lewis River Hydroelectric Projects FERC Settlement Agreement of 2004 and details are outlined in PacifiCorp's most up-to-date Hatchery and Supplemental (H&S) Plan of 2020.

Project Goals

(1) Conduct spawning ground surveys for Chinook salmon in the NF Lewis River downstream of Merwin Dam throughout the entire spawning period. Spawning ground surveys include both weekly mark-recapture surveys for carcasses and peak-count visual surveys of live spawners, carcasses, and redds

(2) Generate an unbiased estimate of the total abundance for Chinook salmon spawners with uncertainty in the NF Lewis River downstream of Merwin Dam

(3) Estimate the composition of spawner abundance by management population (spring, tule, and bright), origin (hatchery, wild), and age (ages 2 – 6)

(4) Evaluate the spatial and temporal spawning distribution of Chinook salmon downstream of Merwin Dam

Methods

A brief description of the survey approach, data collection, and data analysis are outlined below. For a more in-depth description of each aspect of the project, see Bentley et al. (2018) and the annually updated Spawning Ground Survey Protocol for NF Lewis River adult Chinook salmon.

Survey Approach

Spawning ground surveys are conducted for Chinook salmon in the NF Lewis River from the bottom of Eagle Island upstream to just below Merwin Dam (Figure 1), which comprises the entire spawning distribution for Chinook salmon in the mainstem Lewis. Spawning ground surveys typically begin the third week of September (14^{th} – 18^{th}) and generally continue into January to encompass the entire spawning duration of all three populations (i.e., stocks, run types) of Chinook salmon. Surveys are typically conducted 1 – 2 days per week so long as river conditions are conducive to staff safety and fish visibility. One to four jet boats are used to navigate the river and complete spawning ground surveys, which are primarily focused on recovering carcasses to conduct mark-recapture.

Data Collection

During each carcass survey, Chinook salmon carcasses are located, recovered, accessed, sorted, and processed sequentially. All recovered carcasses are enumerated while a subset is sampled for biological data (e.g., fork length – FL –, sex, scales, CWTs) and carcass tagged. Visual surveys are also conducted to count the number of live spawners and redds during the presumed peak spawning periods for all three populations of Chinook salmon. Data are captured on scale cards and whiteboards in the field and entered into WDFW's Traps, Weirs, and Surveys (TWS) Access database. Further data collection and carcass handling protocols are detailed in Bentley et al. (2018).

Data Analysis

Carcass recoveries and associated biological data were queried, summarized, and analyzed to generate estimates of abundance of NF Lewis Chinook salmon using nearly the same methods outlined in Bentley et al. (2018). Briefly, estimates were generated using a multivariate, random-walk mark-recapture Jolly-Seber (J-S) model. Our model was a modified version of the "super-population" Jolly-Seber (J-S) estimator that was developed by Schwarz et al. (1993) and

Schwarz and Arnason (1996) and previously implemented in a Bayesian framework by Rawding et al. (2014). A more detailed description of the data analysis and the J-S model can be found in Appendix A and Appendix B, respectively.

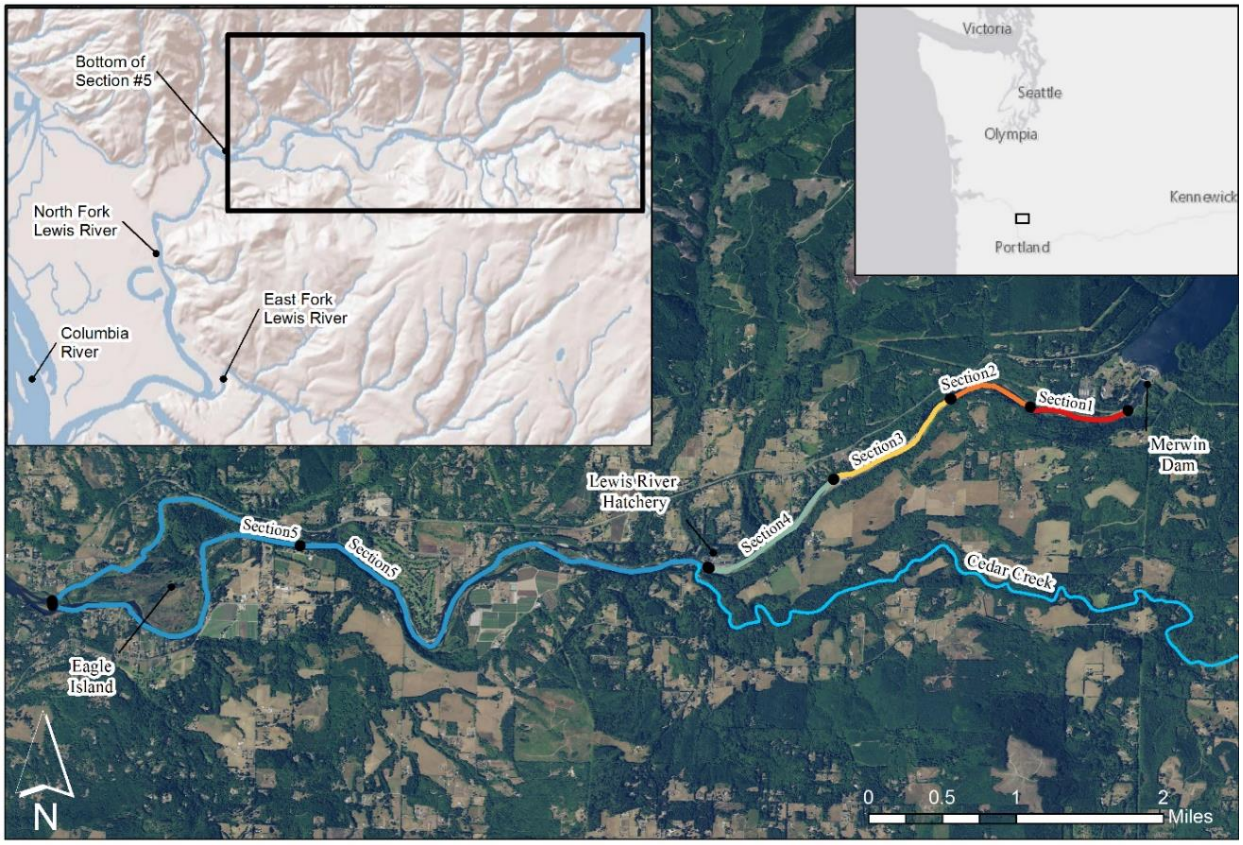

Figure 1. Map of spawning ground survey sections for Chinook salmon in the NF Lewis River.

Results

Data Collection

Mark-recapture carcass tagging surveys were conducted for Chinook salmon in the NF Lewis River downstream of Merwin Dam from September 5th through December 26th, 2023. Surveys began earlier than normal to ensure the entire spring Chinook run was sampled and ended approximately a week earlier than normal as a result of low carcass numbers and survey conditions. In total, 28 individual days were surveyed over 16 weeks and required 47 boat days to complete. Surveys were canceled the week of December 7th due to extremely high flows (>15,000 CFS) and the resulting unsafe conditions.

Across all survey days, a total of 6,262 unique carcasses were recovered of which 2,047 were tagged and 780 were recaptured (Table 1). The total number of carcasses recovered, tagged, and recaptured varied among survey weeks and carcass groupings (Appendix C). Overall, the carcass recoveries were comprised of 51% females, 33% large males, and 6% small males ("jacks").

Table 1. Summary of the total carcass recoveries by grouping, tag status, and recovery rate in 2023.

Carcass Grouping	Maiden	Tagged	Recaptured	Recovery Rate (%)
Jack	389	235	57	24.3
Female	3,163	972	392	40.3
Male	2,710	840	331	39.4
Total	6,262	2,047	780	38.1

Across the entire survey period, the recovery rate of females was slightly higher than the recovery rate for males, and approximately double the recovery rate for jacks (Table 1). However, as observed in previous years, the recovery probability of carcasses varied throughout the fall (Figure 2). In general, recovery probabilities for all sexes (female, large males, and jacks) began relatively low in September before increasing for most of October and November outside of the higher flows and no drawdown during early November. Extremely high flows during the first two and half weeks of December resulted in a missed survey week and a recovery probability of nearly zero during the second week of December. However, reduced flows and a drawdown event during the third week of December resulted in higher-than-normal recovery probabilities, which resulted in hundreds of recoveries, including dozens of recaptures that were originally tagged in November, which was important for deriving a representative dataset.

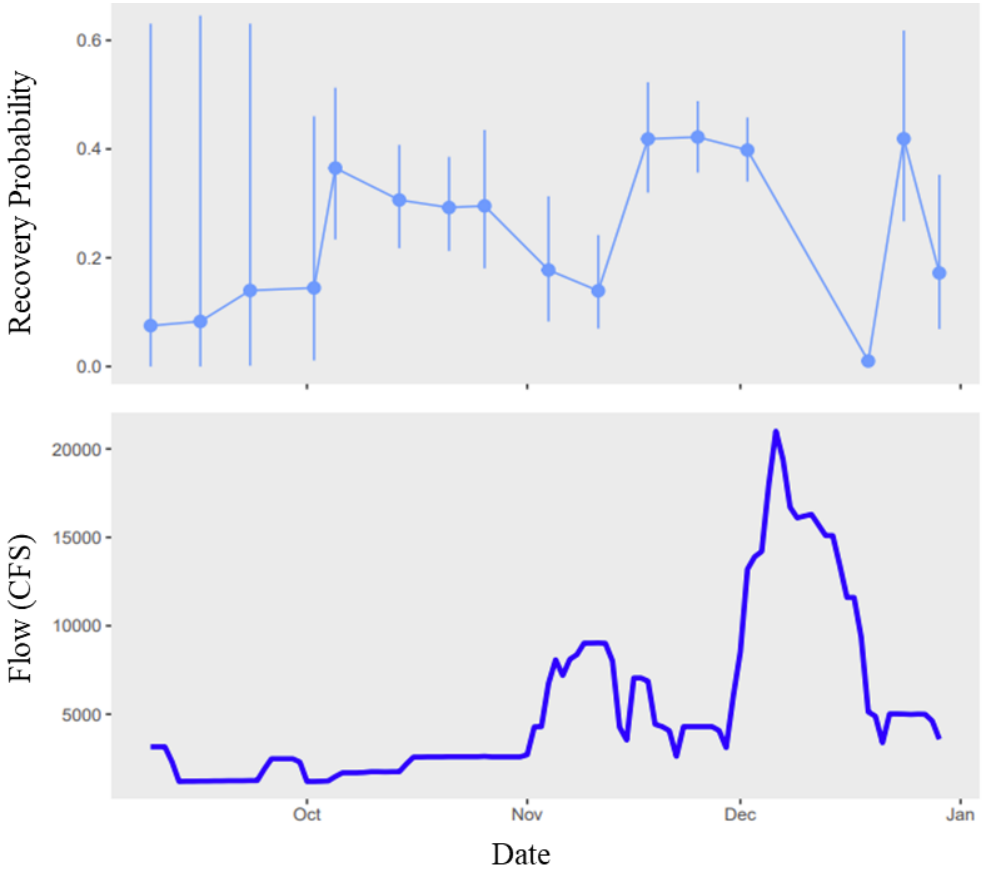

Figure 2. Recovery probability of male carcasses by period (top) and average daily flow below Merwin Dam (bottom) in the fall of 2023. Carcass survey dates are shown with a single dot per week but can be comprised of 1-3 individual survey days.

Abundance and Composition

Estimates of abundance were generated for NF Lewis Chinook salmon for return year 2023 (Table 3 – Table 4). Following two of the highest observed abundances in the past two decades, the estimated number of spring Chinook (mean=109; CV=77% [Table 2]) was both the lowest observed abundance since mark-recapture surveys were re-initiated in 2020 and the lowest since 2017. Tule fall Chinook estimates in 2023 (3,044; 13% [Table 3]) was lower than in 2022 but approximately equal to the average abundance over the previous five years (Figure 3). Bright fall Chinook abundance in 2023 (8,368; 6% [Table 4]) was higher than 2022 but lower than the average abundance over the previous five years (Figure 3).

The proportion of each run that was comprised of hatchery-origin spawners (i.e., pHOS) was 0.74, 0.58, and 0.02, respectively (Table 5). As was previously explained in Bentley et al. (2018), there are no hatchery releases of bright-run Chinook salmon in the lower Columbia Basin. Specifically, the small, estimated proportion of bright-run Chinook that were assigned as hatchery-origin (0.02) is simply an artifact of how biological data are partitioned in the analyses. Thus, the 165 hatchery-origin Chinook that the model estimated as bright-run Chinook are likely hatchery-origin tule-run Chinook.

Table 2. Estimates of abundance (i.e., escapement) and composition for NF Lewis spring-run Chinook salmon in 2023.

Origin	Age	Mean	SD	L95%	Median	U95%	%CV
Hatchery	-	81	62	32	63	260	77
	2	2	3	0	1	7	217
	3	13	12	4	10	43	92
	4	49	38	19	39	152	77
	5	16	16	5	12	59	96
	6	0	1	0	0	2	167
Wild	-	28	25	10	21	95	88
	2	1	3	0	1	7	233
	3	5	6	1	4	18	115
	4	17	15	6	13	54	88
	5	5	6	1	3	19	118
	6	0	0	0	0	1	333
Total	-	109	84	44	84	348	77

Table 3. Estimates of abundance (i.e., escapement) and composition for NF Lewis fall-run Chinook salmon (i.e., tules) in 2023.

Origin	Age	Mean	SD	L95%	Median	U95%	%CV
Hatchery	-	1,763	180	1,369	1,767	2,112	10
	2	28	34	4	18	107	122
	3	309	53	214	306	419	17
	4	1,197	127	921	1,200	1,441	11
	5	225	40	153	223	310	18
	6	4	3	1	3	13	80
Wild	-	1,281	304	871	1,207	2,084	24
	2	59	60	9	42	206	102
	3	203	54	127	194	338	26
	4	850	205	574	799	1,399	24
	5	167	41	103	161	262	24
	6	3	3	-	2	9	88
Total	-	3,044	401	2,312	3,002	3,975	13

Table 4. Estimates of abundance (i.e., escapement) and composition for NF Lewis late fall-run Chinook salmon (i.e., brights) in 2023.

Origin	Age	Mean	SD	L95%	Median	U95%	%CV
Hatchery	-	165	119	66	123	516	72
	2	9	6	2	7	24	68
	3	25	21	9	18	87	83
	4	112	80	44	84	351	72
	5	19	16	6	13	66	86
	6	0	0	0	0	1	131
Wild	-	8,203	424	7,299	8,214	8,998	5
	2	750	101	594	735	986	13
	3	1,132	103	944	1,129	1,344	9
	4	5,478	314	4,820	5,484	6,077	6
	5	829	98	654	825	1,038	12
	6	13	8	2	11	34	65
Total	-	8,368	464	7,422	8,366	9,282	6

Table 5. Estimates of pHOS and pNOS for NF Lewis Chinook salmon by population in 2023.

Population	Variable	Mean	SD	L95%	Median	U95%
Spring	pHOS	0.74	0.06	0.62	0.75	0.84
	pNOS	0.26	0.06	0.16	0.25	0.38
Tule	pHOS	0.58	0.05	0.46	0.6	0.65
	pNOS	0.42	0.05	0.35	0.4	0.54
Bright	pHOS	0.02	0.05	0.01	0.01	0.06
	pNOS	0.98	0.01	0.94	0.99	0.99

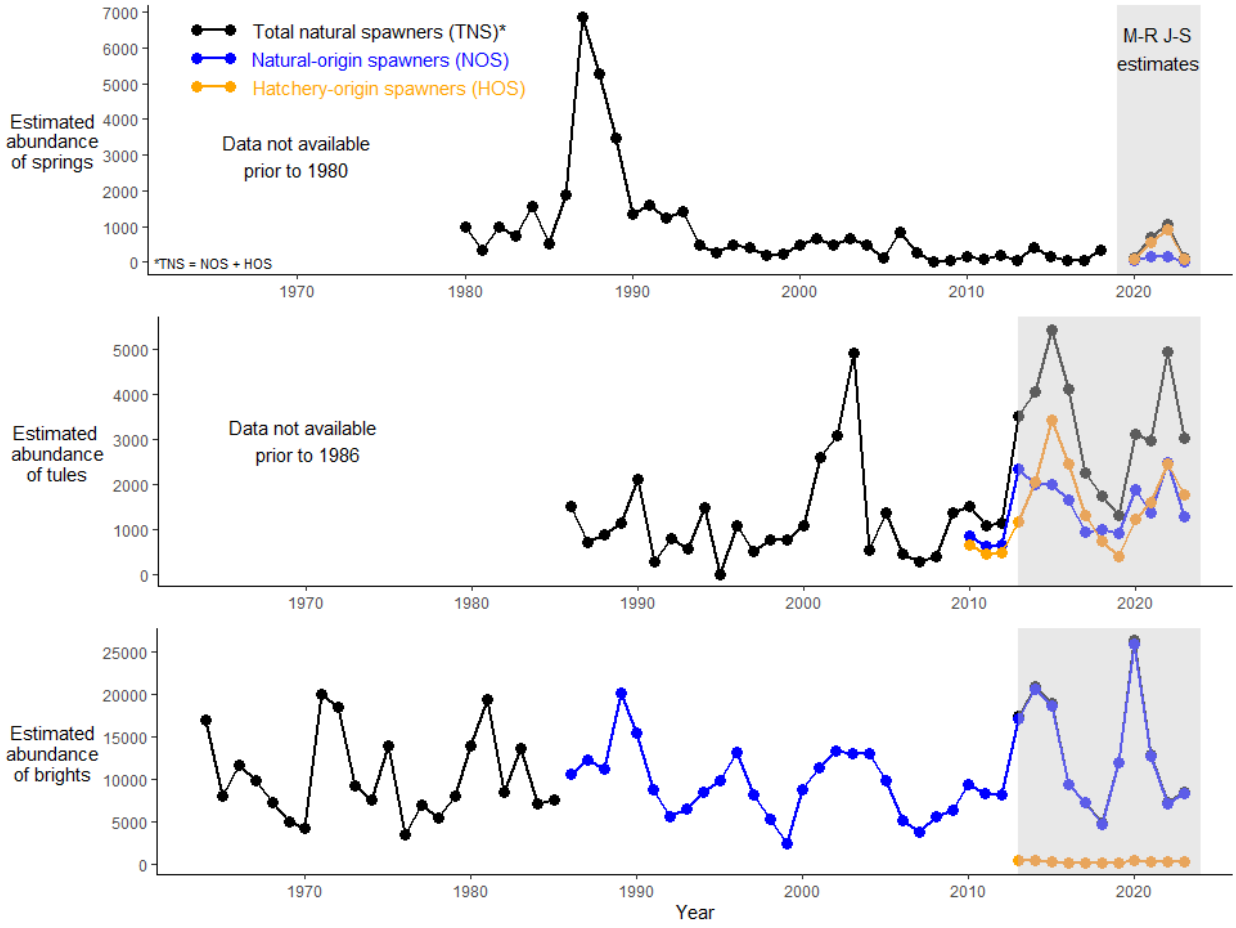

Figure 3. Estimated annual abundance of spring- (top), tule- (middle), and bright-run (bottom) Chinook salmon in the North Fork Lewis River. Total natural spawners (black) are the sum of natural-origin spawners (NOS) and hatchery-origin spawners (HOS). For years in which NOS and HOS abundances were estimated separately, abundances are shown with blue (NOS) and orange (HOS) lines. Mark-recapture Jolly-Seber (M-R J-S) abundance estimates have been used for tules and brights since 2013 (shaded area), and springs since 2020 (details in Bentley et al. 2018). Data were retrieved from WDFW's Salmon Conservation Reporting Engine. Mass marking of Chinook in the lower Columbia was fully implemented and had adults returning in 2010 thereby allowing for NOS and HOS to be differentiated.

Timing and Distribution

Estimates of abundance were generated via a time-stratified model and thus period-specific estimates can be visualized to assess run-timing (Figure 4). Because these data are carcass recoveries, as opposed to live spawners, the observed patterns are a function of relative spawner abundance and recovery probability, which is a function of survey conditions and survey effort. Overall, patterns of run-timing are similar to previous years where spring Chinook are present in the NF Lewis from mid-September through early October with peak carcass abundance in late September, tules are present from mid-September through early November with peak carcass abundance in mid-October, and brights are present from late October through January with peak carcass abundance in late November.

Surveys of live spawners, carcasses, and redds are typically conducted across several weeks corresponding to the peak abundance for each of the three runs. These data have been collected

with the intent of monitoring spawning distribution within and among years. For these surveys to be successful, flows must be relatively low (<5,000 CFS) and clarity high. In 2023, there were a total of nine peak count surveys, but these data are not included here.

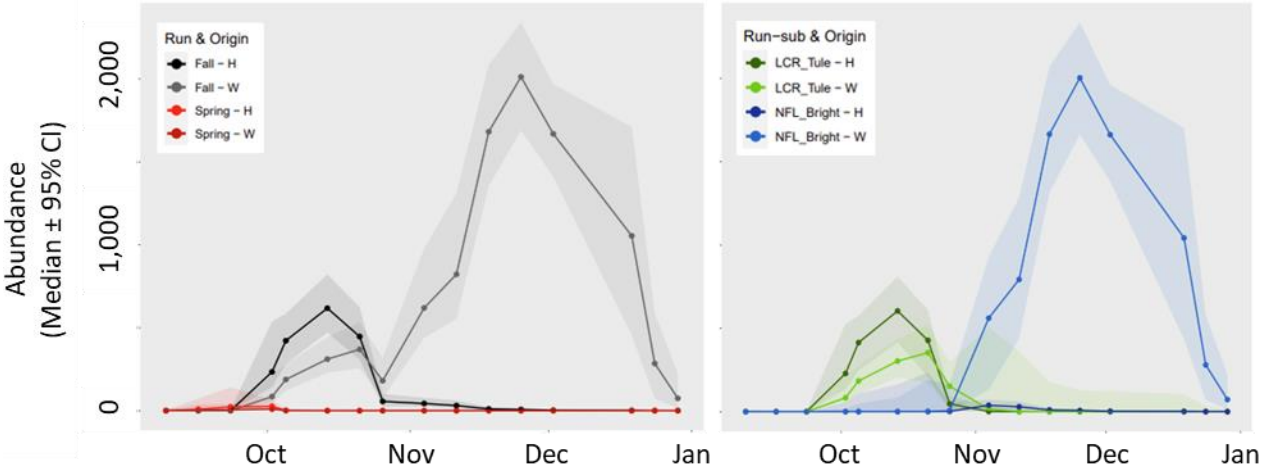

Figure 4. Weekly estimated abundance of A) spring- (red), and fall- (black) run Chinook in the NF Lewis River, 2023, separated by origin and B) the breakdown of tule (green) and bright (blue) runs during the fall-run Chinook season, separated by origin. The relative abundance shown here is based on carcass recoveries and represents the timing of when spawners died.

Assessment and Recommendations

In 2023, as in previous years, the WDFW field crew implemented the data collection protocol as outlined in the study design. At a high level, each week, crews are expected to survey the entire study area, attempt to recover every carcass that was observed, and tag as many carcasses as possible. This approach has resulted in a high absolute and relative number of carcasses being recovered, sampled, and tagged. Specifically, over the past 11 years (2013 – 2023), an average of ~1,300 maiden tule-run carcasses and ~7,500 bright-run carcasses have been recovered, which on average represents ~40% - 60% of the estimated total return, respectively. Similarly, over the same time period, an average of ~500 tule-run carcasses and ~1,900 bright-run carcasses have been tagged, which on average represents ~14% - 18% of the estimated total return, respectively. While these high absolute recoveries and tag numbers have resulted in highly precision estimates of abundance, there can be diminishing returns with regard to mark-recapture-derived estimates. A preliminary analysis of the past 11 years of mark-recapture data for NF Lewis Chinook, demonstrates that the precision of the estimated abundance does not change much once ~500 – 1,000 carcasses are tagged (Figure 5). Therefore, a more thorough evaluation of these mark-capture data should be completed as soon as possible with the goal of providing updated sampling guidance that strives to continue to meet precision targets while minimizing excess sampling effort.

Since 2013, estimates of abundance have been generated for NF Lewis Chinook via mark-recapture carcass surveys. The mark-recapture methods have been evaluated numerous times and the estimates of abundance have been deemed robust (i.e., unbiased/accurate) as a result of a sound study design and the ability to satisfy the assumptions of the mark-recapture estimator.

Estimates of abundance are partitioned by population (spring, tule, fall), origin (hatchery, wild), and age using stratified biological data. As discussed in Bentley et al. (2018) and our Spawning Ground Protocol, partitioning the total estimate by population requires the use of visual stock identification (VSI) to differentiate spring- and fall-run Chinook and the ratio of CWT recoveries to split tules and brights. In short, the resulting estimates of abundance by population assume the VSI and CWT approach generally results in accurate partitioning of the total estimated abundance. Although there are known limitations to these methods, there has been minimal concern over the potential bias that may be induced due to the violation of assumptions because of the low absolute abundance of spring Chinook, and particularly wild-origin adults, and the limited temporal overlap of tules and brights. However, as we have recommended previously, these assumptions should continue to be assessed each year and updated when/if improved methods are available.

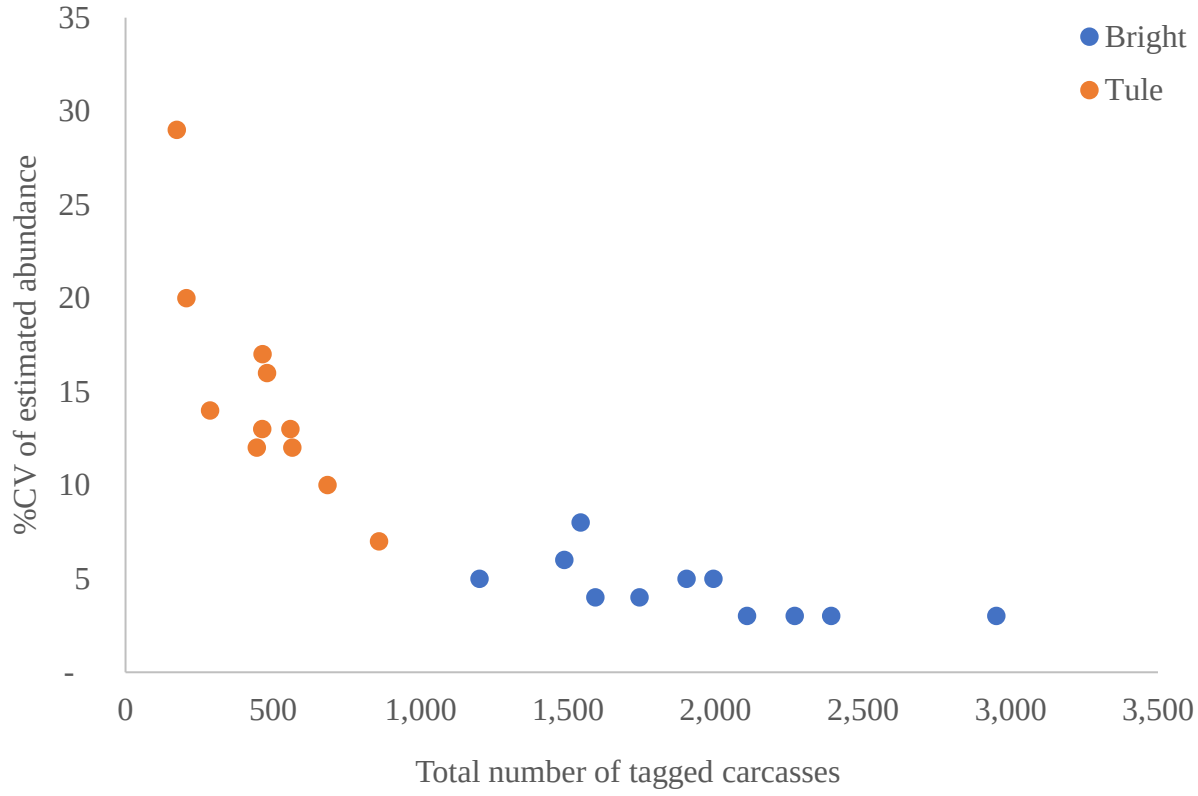

Figure 5. The precision of the estimated abundance for fall-run Chinook, as measured via %CV (coefficient of variation) as a function of the total number of carcasses tagged for mark-capture separated by tule- and bright-run populations. Each point represents data for a single year from 2013 – 2023.

Using data from 2023, we completed a preliminary evaluation of the VSI assignment approach and found that the method provided inaccurate results. Specifically, we used CWT+ carcasses to compare the VSI-based assignment versus the actual run/population assignment based on the recovered CWT that was read in the laboratory. Overall, the VSI-based assignment matched the CWT-based assignment in 32 out of the 39 (82%) CWT+ carcasses recovered throughout the entire 2023 sampling season. However, we found that only 10 of 17 (59%) CWT+ carcasses

were accurately assigned using VSI the last week of September and the first two weeks of October, which is the timing when we expect overlap between spring- and fall-run Chinook to be highest (i.e.,). Given the relatively low sample sizes, we did not attempt to correct the VSI-based run/population assignment during the analysis. However, these results emphasize the need to further evaluate the current VSI-based approach and/or update it with a more accurate method. For instance, as previously mentioned, WDFW commenced a genetic baseline re-assessment for Lower Columbia River Chinook salmon in 2022. One of the main goals of the project is to access the population structure of Chinook in the NF Lewis and evaluate our ability to differentiate these stocks using genetic markers. This work is ongoing but we anticipate preliminary results soon. Overall, this project will greatly enhance our understanding of Chinook genetic structure and could potentially provide an improved method for generating compositional estimates of abundance for NF Lewis Chinook.

References

Bentley, K., Rawding, D., Hawkins, S., Holowatz, J., Nelsen, S., Grobelny, J., and Buehrens, T. 2018. Estimates of escapement and an evaluation of abundance methods for North Fork Lewis River fall-run Chinook salmon, 2013-2017. Washington Department of Fish and Wildlife, FPT 18-03. 86pp. https://wdfw.wa.gov/publications/02004

Gilks, W.R. 2005. Markov Chain Monte Carlo. In Encyclopedia of Biostatistics. John Wiley & Sons, Ltd. doi:10.1002/0470011815.b2a14021.

Laake, J.L. 2013. RMark: An R Interface for Analysis of Capture-Recapture Data with MARK. AFSC Processed Rep 2013-01, 25p. Alaska Fish. Sci. Cent., NOAA, Natl. Mar. Fish. Serv., 7600 Sand Point Way NE, Seattle WA 98115.

Plummer, M. 2007. JAGS: A program for analysis of Bayesian graphical models using Gibbs sampling. In Proceedings of the 3rd International Workshop on Distributed Statistical Computing (DSC 2003). March. pp. 20–22. Available from http://www.ci.tuwien.ac.at/Conferences/DSC-2003/Drafts/Plummer.pdf [accessed 7 January 2015].

R Core Team (2022). R: A language and environment for statistical computing. R Foundation for Statistical Computing, Vienna, Austria. URL https://www.R-project.org/.

RStudio Team (2022). RStudio: Integrated Development Environment for R. RStudio, PBC, Boston, MA URL http://www.rstudio.com/.

Rawding, D., Glaser, B., and Buehrens, T. 2014. Lower Columbia River fisheries and escapement evaluation in southwest Washington, 2010. Washington Department of Fish and Wildlife, FPT 14-10. 289 pp. https://wdfw.wa.gov/publications/01702

Schwarz, C.J., and Arnason, A.N. 2006. Jolly-Seber models in MARK. In Program MARK: A gentle introduction, fifth edition. Edited by E. Cooch and G. White. pp. 401–452. Available from http://www.phidot.org/software/mark/docs/book.

Schwarz, C.J., Bailey, R.E., Irvine, J.R., and Dalziel, F.C. 1993. Estimating Salmon Spawning Escapement Using Capture–Recapture Methods. Can. J. Fish. Aquat. Sci. 50(6): 1181–1197.

Su, S., and Yajima, M. 2021. R2jags: A Package for Running JAGS from R. Available from https://cran.r-project.org/web/packages/R2jags/index.html.

Appendices

Appendix A – Description of Data Analysis

Carcass survey data were queried from the TWS Access database and ran through a standardized set of summarizations in R (R Core Team 2022) via RStudio (RStudio Team 2022). Briefly, each tagged carcass was first designated as either a jack (i.e., males <60 cm), female, or male (males ≥60) based on field calls and/or associated biological data. Capture histories were then generated for each tagged carcass and mark-recapture (M-R) summary statistics were generated by carcass grouping (jack, female, male) and survey period/week using the R package *RMark* (Laake 2013). Biological data were summarized by carcass grouping and survey period/week where visual-stock identification was used to partition spring- and fall-run carcasses, coded-wire tag (CWT) recoveries were used to partition tule and bright run carcasses, adipose clip and CWT status were paired to identify and partition hatchery- and natural-origin carcasses, and scale-age readings were used to partition carcasses into total age 2 – 6.

Estimates of abundance were generated using the "super-population" Jolly-Seber (JS) estimator that was developed by Schwarz et al. (1993) and Schwarz and Arnason (1996) specifically for estimating salmon spawning escapement using mark-capture methods. The super-population JS model has been previously implemented in a Bayesian framework by WDFW and a comprehensive description of the model, including summary statistics, fundamental parameters, derived parameters, and likelihoods, is provided in Rawding et al. (2014). Previously model selection had compared four versions of this model, each with a time-dependent probability of entry, but with combinations of either time-dependent or constant probabilities of survival and capture. A limitation of this approach was that the model with both time-dependent capture and survival probabilities had a considerably larger parameter count, and therefore greater variance, and could not be implemented without first pooling capture periods (thereby inducing bias) if the raw data lacked sufficient statistics for identifiability without pooling.

To address these limitations, in 2020, we modified the fully time-dependent version of the model (a.k.a. the "*ttt*" model). Specifically, the period-specific probabilities of survival (*phi*) and capture (*p*) were estimated using logit-normal random walks while the probability of entry (*pent*) was estimated via a softmax construction and subject to a simplex constraint where the log-components followed a random walk except for the first period, which by convention is fixed to 0. Additionally, the model was modified so that it could generate separate capture, survival, and entry probabilities for distinct groups of fish (e.g., jack, female, and male salmon), but rather than estimate their parameters entirely independently, it was assumed that temporal evolution in their probabilities of entry, survival, and capture might be correlated. Therefore, the process errors of their random walks were estimated via a multivariate-normal distribution with an inverse Wishart prior, allowing the model to estimate the extent of covariance in parameter evolution among the groups of fish. In contrast to the previous model version, this improved super-population JS model enables estimation of the full-rank time-dependent model regardless of data sparsity by enforcing parsimony through random effects "shrinkage"; probabilities of survival, capture, and entry experience shrinkage by modeling the period-to-period differences in as a random effect (i.e., a random walk model is a random-effects model on first-order differences). Definitions of the data, stochastic parameters, and derived parameters that

comprise the model are outlined in Table A-1, Table A-2, and Table A-3, respectively. Model code is shared in Appendix B.

Samples from the posterior distribution were obtained using Markov chain Monte Carlo (MCMC) simulations (Gilks 2005) in JAGS (Plummer 2007) using the R2jags package (Su and Yajima 2021). We ran four chains with 4,000,000 iterations, a burn-in period of 2,000,000, and a thinning rate of 800 so that the number of independent samples, as measured by effective sample size (ESS), was approximately 10,000 for each parameter of interest. Initial values for each chain were automatically generated within the JAGS package. Modeled convergence was assessed in the same manner as the JS models (i.e., assessment of ESS and BGR statistics).

Table A-1. Notation and definition of data used in the updated Jolly-Seber model.

Statistic	Definition
s	number of sample periods (note: each period denoted with an "i"; i = 1, …, s)
num_strata	number of carcass groupings (note: each grouping denoted with a "k"; k = 1, …, num_strata)
$time_i$	Amount of time (e.g., days) between subsequent periods (e.g., $time_i$ = time between $period_{i+1}$ and $period_i$); length of $time_i$ = s-1
$u_{i,k}$	number of carcasses that were handled per period that were unmarked (i.e., maiden captures)
$m_{i,k}$	number of carcasses that were handled per period that were previously marked (i.e., recaptures)
$n_{i,k}$	total number of carcasses that were handled per period (i.e., n = m + u)
$R_{i,k}$	number of carcasses that were marked and released back into the sample area per period (i.e., new marks deployed; subset of n)
$r_{i,k}$	Total number of marked carcasses from each specific period that were subsequently recaptured in any period after release (i.e., number of "R" that are recaptured)
$T_{i,k}$	number of previously marked carcasses that are recaptured during or after a given period (T = m + z; z = number of previously marked carcasses that are recaptured after
$uTot_k$	total number of unmarked carcasses handled across all sample periods (i.e., sum of "u")
ex_tule_i	number of examined carcasses that were tules by period (note: current parameterization does NOT split up race bio-data by "strata" - not enough data)
ex_race_i	number of carcasses examined for race by period (note: current parameterization does NOT split up race bio-data by "strata" - not enough data)
$ex\_clip_{i,k}$	number of examined carcasses that were adipose clipped by period
$ex\_adfin_{i,k}$	number of carcasses examined for adipose clip status by period
$age\_dat_{i,k,1:num\_ages}$	number of examined carcasses by age and period
$age\_tot_{i,k}$	number of carcasses with a specified (read) age by period
num_ages	Number of age groups

Table A-2. Notation and definition of stochastic (a.k.a. fundamental) parameters used in the updated Jolly-Seber model.

Parameter	Definition
inv_Sigma_p	prior on process error variance/covariance matrix for p
inv_Sigma_phi	prior on process error variance/covariance matrix for phi
inv_Sigma_pent	prior on process error variance/covariance matrix for pent
$logit\_p_{1,k}$	prior on p (probability of capture) in the first period
$logit\_phi_{1,k}$	prior on phi (probability of survival) in the first period
$log\_delta_{1,k}$	prior on delta (probability of entry) in the first period
$logit\_p_{i,k}$	prior on p for periods 2:s
$logit\_phi_{i,k}$	prior on phi for periods 2:s
$log\_delta_{i,k}$	prior on delta for periods 2:s
$sigma\_lambda_k$	prior on shape and rate parameters for gamma distribution prior on total abundance (note: shape = rate = sigma_lambda^-2)
$v_{i,k}$	probability that a carcass that was handled in a given period will be marked and re-released back into the sample area
$Ntot_k$	continuous total abundance
$Nsuper_k$	discrete total abundance
inv_Sigma_pclip	prior on process error variance/covariance matrix for pclip
$logit\_ptule_1$	prior on ptule (portion of carcasses that were tule) in the first period
$logit\_pclip_{1,k}$	prior on pclip (portion of carcasses that were clipped) in the first period
$log\_delta\_age_{1,k,a}$	prior on delta_age (age distribution of carcasses) in the first period
$logit\_ptule_i$	prior on ptule for periods 2:s
$logit\_pclip_{i,k}$	prior on pclip for periods 2:s
$log\_delta\_age_{i,k,a}$	prior on delta_age for periods 2:s
$sigma\_ptule_i$	process error standard deviation for ptule
sigma_p.age	process error standard deviation for p.age

Table A-3. Notation and definition of derived parameters used in the updated Jolly-Seber model.

Parameter	Definition
$p_{i,k}$	probability that a carcass will be handled (i.e., captured) for a given period given that it is in the sample area
$phi_{i,k}$	probability that a carcass that is in the sample area for given period will remain (i.e., survive) in the sample area until the following sample period
$pent_{i,k}$	probability that a carcass enters the sample area between subsequent periods (i.e., the fraction of the total number of carcasses that enter the sample area between each period)
$psi_{i,k}$	probability that a carcass enters the sample area, is still available for capture, and is not seen before a specific period; $psi_{1,k} = pent_{1,k}$
$lambda_{i,k}$	probability that a carcass that has been captured will be captured again (i.e., recaptured); $lambda_{s,k} = 0$
$Bstar_{i,k}$	number of carcasses that enter the sample area between two subsequent sample periods (note: these include animals that enter and "leave" before the next sampling period)
$delta_{i,k}$	odds of entering in period
$temp_{i,k}$	probability of recovery = probability of survival ($phi_{i,k}$) X probability of capture ($p_{i,k}$)
$psiPtot_k$	overall probability of recovery a carcass in the sample area across all periods
$multP_{i,k}$	proportion of maiden captures in each period
$tau_{i,k}$	conditional probability that a carcass is recaptured during a specific period given that it was recaptured at or after that sampled period
$Sigma\_p_{k,k}$	Covariance matrix for p process errors; Inverse of "inv_sigma_p"
$Sigma\_phi_{k,k}$	Covariance matrix for phi process errors; Inverse of "inv_sigma_phi"
$Sigma\_pent_{k,k}$	Covariance matrix for pent process errors; Inverse of "inv_sigma_pent"
$sigma\_p\_process_k$	process error standard deviation for p
$sigma\_phi\_process_k$	process error standard deviation for phi
$sigma\_pent\_process_k$	process error standard deviation for pent
$rho\_p_{k,k}$	among strata process error correlation in p
$rho\_phi_{k,k}$	among strata process error correlation in phi
$rho\_pent_{k,k}$	among strata process error correlation in pent
$ptule_i$	proportion of total abundance that was of the run type tule (opposed to bright) by period
$pclip_{i,k}$	proportion of total abundance that was adipose clipped (opposed to UM - adipose intact) by period
$p.age_{i,k,a}$	proportion of total abundance that was of age "a" by period
$Sigma\_pclip_{k,k}$	Covariance matrix for the "pclip" process errors; Inverse of "inv_sigma_p"
$Sigma\_pclip\_process_k$	process error standard deviation for pclip
$rho\_pclip_{k,k}$	among strata process error correlation in pclip
$delta\_age_{i,k,a}$	odds of the age distribution in carcasses' by period

Appendix B – Code for the Multivariate, Random-Walk Mark-Recapture Jolly-Seber Model

```
model{
#-----------------------
#Derived parameters
#-----------------------
Sigma_p<-inverse(inv_Sigma_p)
Sigma_phi<-inverse(inv_Sigma_phi)
Sigma_pent<-inverse(inv_Sigma_pent)
for(k in 1:num_strata){
  pent[1,k]<-1/(1+sum(delta[1:(s-1),k]))
  psi[1,k]<-pent[1,k]
  lambda[s,k] <- 0
  psiPtot[k] <- sum(temp[1:s,k])
  Bstar[1:s,k] ~ dmulti(pent[1:s,k], Nsuper[k])
  for (i in 1:(s-1)){
    phi[i,k] <- ilogit(logit_phi[i,k]) ^ time[i]
    delta[i,k]<-exp(log_delta[i,k]) * time[i]
    psi[i+1,k] <- psi[i,k]*(1-p[i,k])*phi[i,k] + pent[i+1,k] *(phi[i,k]-1)/log(phi[i,k])
    lambda[i,k] <- phi[i,k]*(p[i+1,k]+(1-p[i+1,k])*lambda[i+1,k])
  }
  for(i in 2:s){
    pent[i,k]<-delta[i-1,k]/(1+sum(delta[1:(s-1),k]))
  }
  for (i in 1:s){
    p[i,k] <- ilogit(logit_p[i,k])
    temp[i,k] <- psi[i,k]*p[i,k]
    multP[i,k] <- temp[i,k]/sum(temp[1:s,k])
    tau[i,k] <-p[i,k]/(p[i,k]+(1-p[i,k])*lambda[i,k])
  }
  #calculate process error variance and correlation matrix
  sigma_phi_process[k] <- sqrt(Sigma_phi[k,k])
  sigma_p_process[k] <- sqrt(Sigma_p[k,k])
  sigma_pent_process[k] <- sqrt(Sigma_pent[k,k])
  for (j in 1:num_strata){
    rho_phi[k,j] <- (Sigma_phi[k,j]/(sigma_phi_process[k]*sigma_phi_process[j]))
    rho_p[k,j] <- (Sigma_p[k,j]/(sigma_p_process[k]*sigma_p_process[j]))
    rho_pent[k,j] <- (Sigma_pent[k,j]/(sigma_pent_process[k]*sigma_pent_process[j]))
  }
}
#------
#priors
#------
for(k in 1:num_strata){
  sigma_lambda[k] ~ dt(hyper_value_sigma_lambda_mu, hyper_value_sigma_lambda_sd^-2, 1) T(0,)
  #nuisance variable to detect if n>0
  for (i in 1:s){
    v[i,k] ~ dbeta(hyper_value_beta_v, hyper_value_beta_v)
  }
  #Priors for first states in process model of prob capture, survival, birth:
  logit_phi[1,k] ~ dnorm(hyper_value_logit_phi_1_mu, hyper_value_logit_phi_1_sd^-2)
  logit_p[1,k]   ~ dnorm(hyper_value_logit_p_1_mu,   hyper_value_logit_p_1_sd^-2)
  log_delta[1,k] ~ dnorm(hyper_value_log_delta_1_mu, hyper_value_log_delta_1_sd^-2)
```

```
  #priors on abundance
  Ntot[k] ~ dgamma(sigma_lambda[k]^-2, sigma_lambda[k]^-2)
  Nsuper[k] ~ dpois(Ntot[k])
}
#process model priors
for (i in 2:(s-1)){
  logit_phi[i,1:num_strata] ~ dmnorm(logit_phi[i-1,1:num_strata], inv_Sigma_phi)
  log_delta[i,1:num_strata] ~ dmnorm(log_delta[i-1,1:num_strata], inv_Sigma_pent)#similar to dirichlet
trick except used additive log ratios
}
for(i in 2:s){
  logit_p[i,1:num_strata] ~ dmnorm(logit_p[i-1,1:num_strata], inv_Sigma_p)
}
#priors for process error covariance matrices
inv_Sigma_p    ~ dwish(Rmat[1:num_strata,1:num_strata],num_strata + 1)
inv_Sigma_phi  ~ dwish(Rmat[1:num_strata,1:num_strata],num_strata + 1)
inv_Sigma_pent ~ dwish(Rmat[1:num_strata,1:num_strata],num_strata + 1)
#-----------
#Likelihoods
#-----------
for(k in 1:num_strata){
  uTot[k] ~ dbin(psiPtot[k],Nsuper[k])
  u[1:s, k] ~ dmulti(multP[1:s,k],uTot[k])
  for (i in 1:(s-1)){
    R[i,k] ~ dbin(v[i,k], n[i,k])
    r[i,k] ~ dbin(lambda[i,k],R[i,k])
  }
  for (i in 2:(s-1)){
    m[i,k] ~dbin(tau[i,k],T[i,k])
  }
}
#~~~~~~~~~~~~~~~~~~~~~~~~~~~~~~~~~~~~~~~~~~~~~~~~~~~~~~~~~~~~~~~~~~~~~~~~~~~~~~~~~~~~~~~~~~~~~~~~~~~~
#         Partition Bstar estimates by proportional data: race, clips, sex and age
#~~~~~~~~~~~~~~~~~~~~~~~~~~~~~~~~~~~~~~~~~~~~~~~~~~~~~~~~~~~~~~~~~~~~~~~~~~~~~~~~~~~~~~~~~~~~~~~~~~~~
#derived
Sigma_pclip<-inverse(inv_Sigma_pclip)
for(i in 1:s){
    ptule[i] <- ilogit(logit_ptule[i])
    pfall[i] <- ilogit(logit_pfall[i])
}
for(k in 1:num_strata){
sigma_pclip_process[k] <- sqrt(Sigma_pclip[k,k])
  for (j in 1:num_strata){
    rho_pclip[k,j] <- (Sigma_pclip[k,j]/(sigma_pclip_process[k]*sigma_pclip_process[j]))
  }
  for(i in 1:s){
    pclip[i,k] <-ilogit(logit_pclip[i,k])
    for(a in 1:num_ages){
      delta_age[i, k, a] <- exp(log_delta_age[i,k,a])
      p.age[i, k, a] <- delta_age[i,k,a]/sum(delta_age[i,k,1:num_ages])
    }
  }
}
#priors
```

```
inv_Sigma_pclip ~ dwish(Rmat[1:num_strata,1:num_strata],num_strata + 1)
sigma_ptule ~ dt(hyper_value_sigma_ptule_mu,hyper_value_sigma_ptule_sd^-2,1) T(0,)
sigma_pfall ~ dt(hyper_value_sigma_pfall_mu, hyper_value_sigma_pfall_sd^-2,1) T(0,)
sigma_p.age  ~ dt(hyper_value_sigma_p.age_mu,hyper_value_sigma_p.age_sd^-2,1) T(0,)
for(i in 2:s){
  logit_ptule[i] ~ dnorm(logit_ptule[i-1],sigma_ptule^-2)
  logit_pfall[i] ~ dnorm(logit_pfall[i-1],sigma_pfall^-2)
  logit_pclip[i,1:num_strata] ~ dmnorm(logit_pclip[i-1,1:num_strata],inv_Sigma_pclip)
}
logit_ptule[1] ~ dnorm(hyper_value_logit_ptule_1_mu, hyper_value_logit_ptule_1_sd^-2)
logit_pfall[1] ~ dnorm(hyper_value_logit_pfall_1_mu, hyper_value_logit_pfall_1_sd^-2)
for(k in 1:num_strata){
  logit_pclip[1,k] ~ dnorm(hyper_value_logit_pclip_1_mu, hyper_value_logit_pclip_1_sd^-2)
  for(a in 1:num_ages){
    log_delta_age[1, k, a] ~ dnorm(hyper_value_log_delta_age_1_mu,hyper_value_log_delta_age_1_sd^-2)
    for(i in 2:s){
      log_delta_age[i, k, a] ~ dnorm(log_delta_age[i-1, k, a],sigma_p.age^-2)
    }
  }
}
#Likelihoods
for(k in 1:num_strata){
  for(i in 1:s){
    ex_clip[i, k] ~ dbin(pclip[i, k],ex_adfin[i, k])
    age_dat[i, k, 1:num_ages] ~ dmulti(p.age[i, k, 1:num_ages], age_tot[i, k])
}
for(i in 1:s){
    ex_tule[i] ~ dbin(ptule[i], ex_race[i])
    ex_fall[i] ~ dbin(pfall[i], ex_run[i])
}
}
```

Appendix C – Summarized mark-recapture recovery data by carcass grouping

Table C-1. Summary of mark-recapture statistics by date/period for the **jack** carcass grouping in 2023.

Period	Date (mm-dd)	Handled (n_i)	Maidens (u_i)	Tagged (R_i)	Recaptures in a period (m_i)	Recaptures from a release (r_i)	Eventual recaps at large (z_i)	Percent recaptured (r_i/R_i)
1	9/5	0	0	0	0	0	0	-
2	9/12	0	0	0	0	0	0	-
3	9/19	1	1	1	0	0	0	0%
4	9/28	1	1	0	0	0	0	-
5	10/3	2	2	2	0	0	0	0%
6	10/10	3	3	3	0	0	0	0%
7	10/17	0	0	0	0	0	0	-
8	10/23	0	0	0	0	0	0	-
9	10/31	11	11	10	0	1	0	10%
10	11/7	12	11	10	1	3	0	30%
11	11/14	68	66	48	2	15	1	31%
12	11/21	167	153	109	14	32	2	29%
13	11/28	159	125	44	34	3	0	7%
14	12/12	0	0	0	0	0	3	-
15	12/20	19	16	8	3	3	0	38%
16	12/26	3	0	0	3	0	0	-
Total	-	446	389	235	57	57	6	24%

Table C-2. Summary of mark-recapture statistics by date/period for the **female** carcass grouping in 2023.

Period	Date (mm-dd)	Handled (n_i)	Maidens (u_i)	Tagged (R_i)	Recaptures in a period (m_i)	Recaptures from a release (r_i)	Eventual recaps at large (z_i)	Percent recaptured (r_i/R_i)
1	9/5	1	1	1	0	0	0	0%
2	9/12	4	4	4	0	2	0	50%
3	9/19	10	8	7	2	1	0	14%
4	9/28	99	98	57	1	34	0	60%
5	10/3	212	183	73	29	28	5	38%
6	10/10	231	199	47	32	11	1	23%
7	10/17	196	188	22	8	9	4	41%
8	10/23	134	122	28	12	8	1	29%
9	10/31	190	181	58	9	14	0	24%
10	11/7	152	142	69	10	39	4	57%
11	11/14	568	530	200	38	116	5	58%
12	11/21	735	623	231	112	103	9	45%
13	11/28	614	506	132	108	21	4	16%
14	12/12	8	8	5	0	1	25	20%
15	12/20	376	350	38	26	5	0	13%
16	12/26	25	20	0	5	0	0	-
Total	-	3,555	3,163	972	392	392	58	40%

Table C-3. Summary of mark-recapture statistics by date/period for the **male** carcass grouping in 2023.

Period	Date (mm-dd)	Handled (n_i)	Maidens (u_i)	Tagged (R_i)	Recaptures in a period (m_i)	Recaptures from a release (r_i)	Eventual recaps at large (z_i)	Percent recaptured (r_i/R_i)
1	9/5	0	0	0	0	0	0	-
2	9/12	0	0	0	0	0	0	-
3	9/19	2	2	2	0	0	0	0%
4	9/28	49	49	31	0	14	0	45%
5	10/3	181	169	64	12	22	2	34%
6	10/10	311	292	66	19	27	5	41%
7	10/17	211	186	24	25	9	7	38%
8	10/23	89	75	20	14	3	2	15%
9	10/31	116	112	39	4	6	1	15%
10	11/7	125	120	62	5	39	2	63%
11	11/14	474	444	169	30	92	11	54%
12	11/21	648	569	209	79	89	24	43%
13	11/28	629	524	135	105	25	8	19%
14	12/12	8	7	3	1	2	32	67%
15	12/20	177	145	16	32	3	2	19%
16	12/26	21	16	0	5	0	0	-
Total	-	3,041	2,710	840	331	331	96	39%